

---

# THERMODYNAMIC ANALYSIS AND MOLECULAR MODELING OF RAPANA VENOSA HEMOCYANIN – FUNCTIONAL UNIT RVH2-E

L. Velkova<sup>1</sup>, P. Dolashka-Angelova<sup>1</sup>, A. Dolashki<sup>2</sup>, W. Voelter<sup>2</sup>, B. Atanasov<sup>1</sup>

<sup>1</sup> Institute of Organic Chemistry, Bulgarian Academy of Sciences, G. Bonchev 9, Sofia 1113, Bulgaria

<sup>2</sup> Interfaculty Institute of Biochemistry, University of Tübingen, Hoppe-Seyler-Straße 4, D-72076 Tübingen, Germany

Correspondence to: Prof. Dr. B. Atanasov

E-mail: boris@orgchm.bas.bg

---

## ABSTRACT

*pH-T diagram is typical “phase portrait” for stability of functional unit RvH2-e. Using different techniques the T-transition curves at different pH for RvH2-e were analyzed and the parameters of the thermodynamic functions were obtained. Increasing temperature and within the T range 25-55°C the reversibility increases and “opens a reversibility window” within the range of pH 5.5-9.0, for which were calculate at standard temperature the thermodynamic functions  $\Delta H^\circ$  and  $\Delta G^\circ_{exp}$ .*

*Molecular modeling of correct 3D structure of functional unit RvH2-e was done which allows us to fix most probably position of missing 9 residues now presented in existed x-ray model at very poor resolution of 3.30Å.*

**Keyword:** Rapana venosa Hemocyanin functional unit RvH2-e, Circular dichroism spectra, Reversible denaturation, Thermodynamic characteristics, 3D- structure

## Introduction

In the hemolymph of many arthropodan and molluscan species oxygen is transported by large copper-containing respiratory proteins, termed hemocyanins (Hcs) (14,16). These proteins bind oxygen reversible at a binuclear active site and transport it to the tissues. The basic quaternary structure of molluscan hemocyanin is a ring-like decameric homo-oligomer, assembled from 10 copies of a ~350- to 400-kDa subunit. In gastropods and bivalves the typical quaternary structure for native hemocyanin is a cylindrical didecamer, formed by face-to-face assembly of two decamers (16). The subunit of gastropod hemocyanin is a ~ 400-kDa polypeptide folded into seven or eight different linked globular functional units (FUs) of Mw ~ 50 kDa, termed at FU-a to FU-h (from the N- to the C-terminus). Each FU contains two copper atoms which can reversibly bind one dioxygen molecule (2). Hemocyanins of the gastropods *Megathura crenulata* (3), *Haliotis tuberculata* (13), and *Rapana venosa* (6) has two distinct native homodecameric forms each containing one of the two subunit isoforms. The association– dissociation properties of molluscan and arthropod Hcs (8-11), together with the conformational stability of Hcs under various physical conditions (i.e. temperature, pH and etc.) (7,11) and/or chemical agents (10-

12) have been studied. However, such studies may be complicated by the fact it may be difficult to distinguish between the effects on the quaternary structure of the oligomeric protein (i.e. initial dissociation) and those on the tertiary and secondary structure (i.e. subunit unfolding), depending upon the dissociation conditions.

The main aim of this study is to determine the reversibility/irreversibility and association/dissociation behaviour of functional unit RvH2-e, isolated from structural subunit RvH2, with respect to pH and temperature using circular dichroism (CD). The narrow range over which the system is irreversible has been determined using two independent ways of denaturation and the corresponding thermodynamic parameters were calculated. The narrow range over which the system is reversible has been determined using two independent ways of denaturation and the corresponding thermodynamic parameters were calculated. At last, precise molecular modeling was performed, justifying position of several missing amino acid residues and thus pave the way for detail theoretical analysis

## Materials and methods

### *Isolation of functional unit RvH2-e from structural subunit RvH2 of Rapana venosa hemocyanin*

*Rapana venosa* hemocyanin (RvH) was isolated from the hemolymph of marine snails living in the Black sea. Native Hc was purified from the hemolymph of *Rapana venosa* Hc as described previously by (12). The molecule of RvH is

organized by two polypeptide structural subunits RvH1 and RvH2 (7). The dissociation of the native Hc was obtained dialyzing the native protein for 24 hours against 0.13 M glycine/NaOH, pH 9.6. The dissociated fractions were separated on an ion-exchange chromatography column of DEAE-Sepharose CL-6B, equilibrated with 50 mM Tris/HCl buffer, 10 mM EDTA, pH 8.2, with a 0.2-0.5 M NaCl gradient. After treatment of the isolated structural subunits RvH1 and RvH2 with trypsin in a ratio of 400:1 and incubation at 37°C, for 4 hours, the tryptic hydrolysate was separated on of an ion exchange “Resource Q 6 ml” (Pharmacia) column using an FPLC system and eluted with 50 mM Tris/HCl buffer, pH 8.2. with a 0.0-0.5 M NaCl gradient as described (7).

### CD measurements

**(A)** Circular dichroism (CD) spectra were recorded in a J-720 spectropolarimeter (Jasco, Tokyo, Japan). Cylindrical temperature-controlled quartz cells with a path length of 10 mm were used in all experiments. CD spectra were recorded in the range between 200 and 250 nm with a bandwidth of 1 nm, a scan speed of 50 nm/min, and a time constant of 8.0 s. Protein solutions in 20 mM Tris/HCl, 10 mM CaCl<sub>2</sub> buffer with different pH values (from 2.5 to 12.0) were thermostatically-controlled using a NESLAB thermostat model RTE-110 connected to a digital programming controller and a thermocouple placed inside the optical cell. Temperature denaturation studies for the samples at different pH (from 1.5 to 12.0) were measured after 20 min incubation. From 15°C up to 95°C the  $[\Theta]_{222}$  values were recorded in intervals of 5±0.2°C.

**(B)** CD spectra of standardized hemocyanin solutions (see above **section A**) were recorded from 190 to 240 nm in a wide interval of pH (2-12, with ~0.5 pH increments) and temperature (20-85°C at 5°C steps). More precisely, the extreme values at 222 nm were digitalized and recalculated in  $[\Theta]_{222}$  (deg.cm<sup>2</sup>.dmol<sup>-1</sup>) units. Two independent sets of experimental data –  $[\Theta]_{222}$  as a function of T°C for 14-15 samples at different pH and  $[\Theta]_{222}$  as a function of pH for 14-15 samples at different T°C – were collected for functional unit RvH2-e. The experimental matrix  $[\Theta]_{\text{exp}}(T)$  was converted to the calculated  $[\Theta]_{\text{cal}}(\text{pH})$  and the matrix  $[\Theta]_{\text{exp}}(\text{pH})$  – to the  $[\Theta]_{\text{cal}}(T)$ . The total reversibility of the system suggests independence of the terminal states from the path(s) of realization. Thus, if our system is reversible, then  $[\Theta]_{\text{cal}}(T)$  curves must be identical as  $[\Theta]_{\text{exp}}(T)$  curves and the  $[\Theta]_{\text{cal}}(\text{pH})$  curves will be identical for  $[\Theta]_{\text{exp}}(\text{pH})$  curves. To prove this strong requirement of reversibility we have

extracted each pair of curves with the same (T, pH)-signatures and plotted these as  $\Delta[\Theta](T)$  and  $\Delta[\Theta](\text{pH})$ . The relative percentage of  $\Delta[\Theta]$  with steps of 4% was used to construct “T-pH phase diagrams” for each of the three proteins within 80-100 % reversibility.

### Estimation of the effective “melting temperatures” ( $T_m$ ) and the “ $T_m$ -pH phase diagram”.

From averaged  $[\Theta]_{\text{exp}}(T)$  curves, neglecting the complexity of the averaged curve and an oversimplified assumption for the “two-state” ( $N \leftrightarrow D$ ) mechanism (crude “zero approximation”), we estimate “melting temperature”  $T_m$  as the temperature of half-denaturation for RvH2-e.  $\Delta H_{\text{eff}} = 4R(273+T^\circ\text{C})^2_{m,n}/1000.\Delta T_n$  (kcal/mol) (15)

The results are plotted as  $T_m(\text{pH})$ . In this case  $T_m$  is used as integral characteristics of a structure containing with the expectation that there will be T/pH-dependent changes in quaternary structure. Our van't Hoff's analysis of these data was made using plots of  $\log K_{\text{obs}}/R$  vs  $1/T$  and calculating  $\Delta G_{\text{vh}} = -RT \ln K_{\text{obs}} = -RT[Y/(1-Y)]$ , where Y is the relative ( $0 < Y < 1$ ) change of  $[\Theta]_{\text{exp}}$  as a function of the temperature (in K).

**Molecular modeling** was done using programs MolIDE (1) and “Swiss Model” (5) on PDB file 1LNL (4). All Ala residues at 9 positions (16, 20, 49, 51, 55, 114, 146, 305 and 329) were substituted with their natural amino acid residues (Arg, His, Tyr, Glu, Arg, Pro, Phe, Arg and Lys respectively) followed by repeated structural “adaptation” using large rotamers library. At last appropriate “clashing analysis” allow us to select most preferred conformers. The positions and orientation of these residues are giving on Fig.4. At last the detail energy calculations on derived models were performed and most stable structure was fixed.

## Results and Discussion

**Influence of temperature on circular dichroism of RvH2-e at different pH values.** An initial feature is the presence of T-induced changes within a wide temperature interval (20-85°C) (as example **Fig.1A**). Secondly, specificity is irreversibility to common “end states” with a relatively similar disordered structure. The amplitude  $\Delta[\Theta]_N - \Delta[\Theta]_D$  for curves at different pH is slightly decreased on moving to extreme pH values. The relatively small changes of initial  $[\Theta]_{222}$  at high temperatures indicate that many structure elements are preserved, especially at neutral pH and even at extreme high temperatures. Thus we have not detected T-dependent unfolding and probably even at temperatures above 90°C the proteins retain a “globule state”.

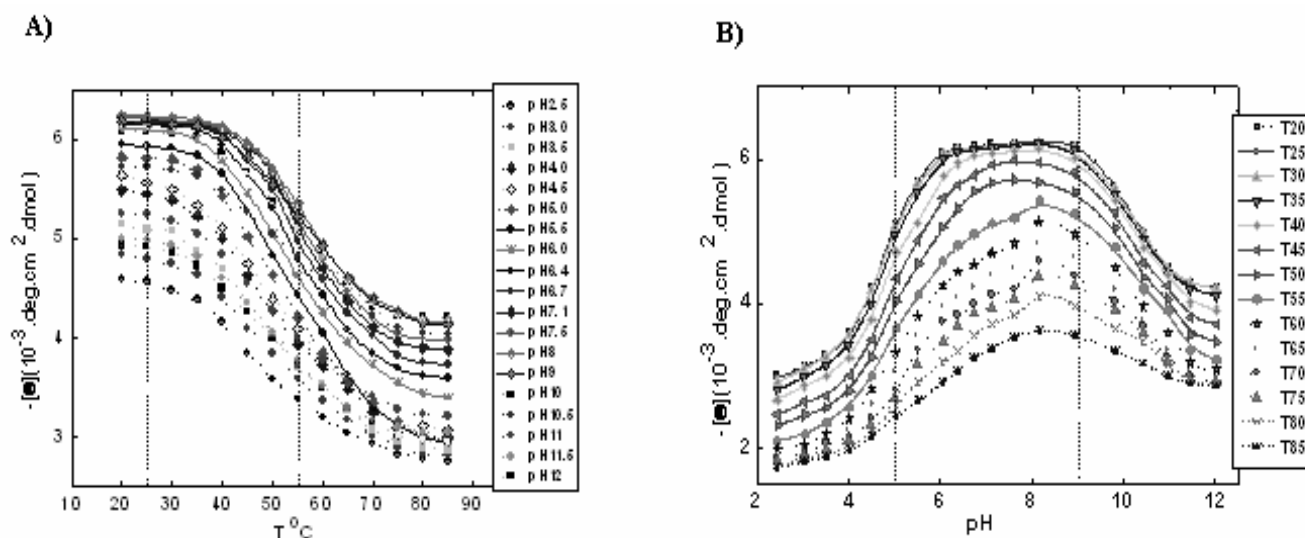


**Fig. 1. A )** Influence of temperature on circular dichroism spectra at different pH values. The T-induced changes are obtained over a wide temperature interval (25-85°C) et fixed pH (2.5-12). Influence of temperatures on  $[\theta]_{222}$  of RvH2-e at different pH. Curves considered to be “reversible” (solid lines) are shown within the two vertical dashed lines. All other curves are irreversible. **B )** Influence of pH on  $[\theta]_{222}$  of RvH2-e at different temperatures. Part of the curves considered to be fully “reversible” (in solid) are presented within vertical dashed lines. All others are irreversible.

### Influence of pH on dichroic spectra of RvH2-e at 222nm at different temperatures

The  $[\theta]_{222}$  vs. pH plots (as example **Fig.1B**) represent a set of smooth and partially “bell shaped” curves with maxima between pH 5-9 and non-symmetric acidic and alkaline extremes, but without any obvious sigmoid feature at extreme pH. In the alkaline part (pH 8-12), relative changes are too small and non-cooperative (within a wide pH interval), indicating that alkaline denaturation cannot be achieved as reversible process. **pH-transitions** (acid and alkaline denaturation) are poorly presented in all the extremes within the data sets of RvH2-e can be accounted for by an increased stability due to quaternary structure. The  $[\theta]_{222}$  /pH within the range of pH6.5-8.5 at a wide plateau is present for low temperatures 20-40°C and the corresponding  $[\theta]_{222}$ (pH) curves are pH-independent. The conclusion is that no titrable groups in this pH region which are resinsible for structural stability.

### Reversibility T-pH - “phase diagram”

Because of the large set of experimental points in the T-pH grid of  $[\theta]_{222}$ , we take “dissections” at a given temperature for discrete pH values and *vice versa* (at given pH for corresponding temperatures) and have converted the data to a new pair of data sets. If the principle of thermodynamic independence of the denaturation state from the way of its

achievement is correct, then we should obtain the same results.

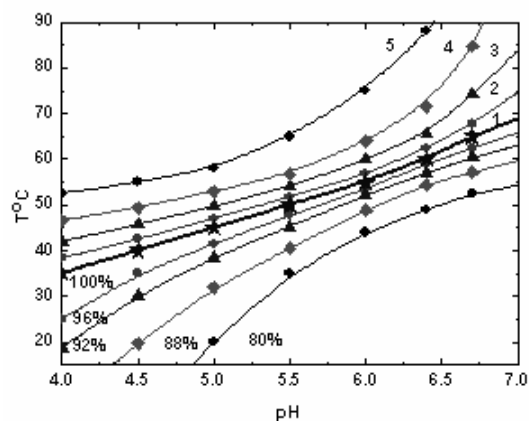


**Fig. 2.** Curves are iso-lines at equal renaturation reversibility of RvH2-e. The surface between to T-pH lines correspond to reversibility (in %) as follow: (1) 100, 96 (2), 92 (3), 88 (4) and (5) lower then 80.

We accept that extension of the relative identity (in %) is a measure and criterion of reversibility (3). The results from this “morphing” for RvH2-e is shown in **Fig.2**. The lines connect T-pH points with equalreversibility (%) as 100 (1), 96 (2), 92 (3), 88 (4) and 80. We propose that this “phase portrait” for reversibility in pH-T perturbations for RvH2-e is valid. As is shown in the case, the reversibility at 25°C is pH the systems is reversible. Increasing temperature and within

the T range 30-55°C the reversibility increases and “opens a window” within the range of pH 5.5 - 9.0.

**Thermodynamic characteristics of T-pH denaturation of RvH2-e.** Demonstration of full reversibility is that all experimental determination  $\Delta H_m$  within the range of pH 5.5-9.0 are located in one straight line. Determinated  $\Delta C_p$  is 550 (cal/mol.grad) from  $\Delta H_m$  vs  $T_{tr}$  – within the range of pH 5.5-9.0 (Fig.3). The large volume  $C_p$  550 cal/mol. grad is in agreement with opening of hydrophobic protein interior at denaturation. Both  $\Delta H^\circ$  and  $\Delta G^\circ_{exp}$  (in kcal/mol) are recalculated for standard temperature 298K within 5.5-9.0 interval. pH-Dependent part of structural stability ( $\Delta G^\circ_{exp}$ ) of

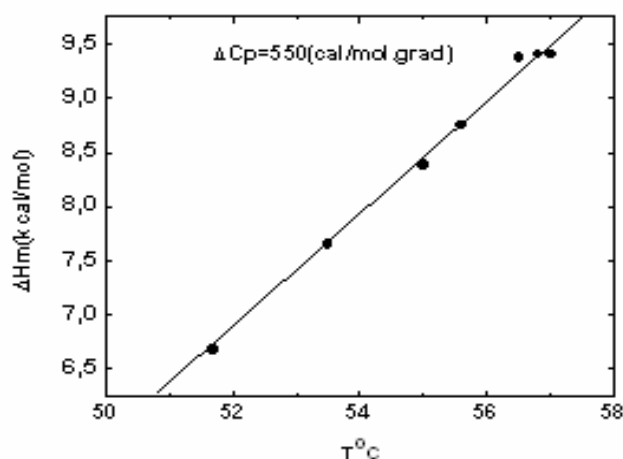


**Fig. 3.** Indirect the determination of specific heat capacity ( $C_p$ ) from  $\Delta H_m$  vs  $T_{tr}$  – within the range of pH 5.5-9.0 of the denaturation process for all pH-s.

**Molecular modeling** of correct 3D structure allows us to fix most probably position of missing 9 residues which was presented at existed x-ray model at very poor resolution of 3.30Å. In their PDB file 1LNL at these positions are only Ala residues (4). Most of them are on the loops and molecular surface which permit high flexibility and this is reason for their poor resolution. Seven of constructed residues are ionic and should have strong participation in pH-dependent stability. And this is especially importantly for His20, which realize contact with the neighbour functional unit. Also great influence of quaternary structure should have the cluster Tyr49–Glu51–Arg55 (**Fig.5**).

Thus the adjusted RvH2-e structure permit to be provided detail electrostatic analysis which to explain number of pH-dependent properties.

reversibly denaturation of RvH2-e [ $\Delta G^\circ_{exp}(pH)$ ] have shape unusual pH-dependent stability curve, which can be theoretically predicted by using appropriate 3D atomic model of RvH2-e. The curve is pH-dependent with complex shape and has total minimum at pH 7.6(Fig.4). The experimentally obtained total stability is -33.4 kcal/mol (**Fig.4**).  $\Delta H^\circ$  was recalculated at standard temperature 298K within the range of pH 5.5-9.0 (determination region reversibility) from  $\Delta H_m$  for each fixing pH-value and was determined that  $\Delta H^\circ$  is pH-independent, has value -8.0 kcal/mol. Because their pH-independency we can address them as processes of hydrophobic rearrangement of the quaternary structure.

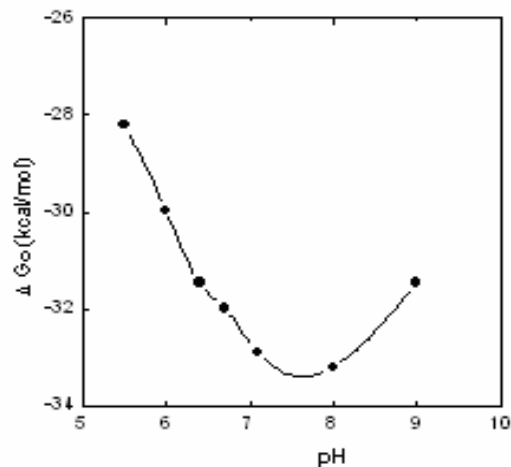


**Fig. 4.** The Gibbs free energy of denaturation at wide pH interval (pH-dependant stability) is calculated with extrapolation  $T = 298$  K. Structural stability ( $\Delta G^\circ_{exp}$ ) of reversibly denaturation of RvH2-e [ $\Delta G^\circ_{exp}(pH)$ ] is pH-dependent.

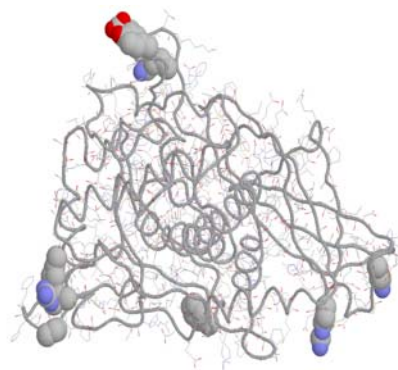


**Fig. 5.** Renewed 3D-atomic structure of RvH2-e with added missed nine amino acid residues.

## Acknowledgments

This work was supported by a research grant TK-01/496 by the Ministry of Sciences and Education of Bulgaria.

## REFERENCES

1. **Canutescu A.A., Dunbrack R.L. Jr.** (2005) Bioinformatics. PMID: 15845657  
[http://dunbrack.fccc.edu/MolIDE\\_download](http://dunbrack.fccc.edu/MolIDE_download)
2. **Cuff M. E., Miller K. I., van Holde K. E.** (1998) *J. Mol. Biol.* **278**, 855-870.
3. **Gebauer W., Harris J. R., Heid H., Süling M., Hiltenbrand R., Söhngen S., Wegener-Strake A., Markl J.** (1994) *Zoology* **98**, 51-68.
4. **Georgieva D., Schwark D., Nikolov P., Idakieva K., Parvanova K., Dierks K., Genov N., Betzel C.** (2005) *Biophys J.* **88**, 1276-82.
5. **Guex, N., Peitsch, M.C.** (1997). *Electrophoresis* **18**, 2714-2723.
6. **Dolashka-Angelova P., Schick M., Stoeva S., Voelter W.** (2000b) *Int. J. Biochem. & Cell Biology* **32**, 529-538
7. **Dolashka-Angelova P., Schwarz H., Dolashki A., Beltramini M., Salvato B., Schick M., Saeed M., Voelter W.** (2003) *Biophys. Acta* **1646**, 77-85.
8. **Dolashka-Angelova. P., Hristova R., Stoeva S., Voelter W.** (1999) *Spectrochim. Acta* **55**, 2927-2934.
9. **Dolashka-Angelova P., Stoeva S., Hristova R., Schuetz J., Beltramini M., Salvato B., Schwartz H., Voelter W.** (1999) *Curr. Topics Peptide & Prot. Res.* **3**, 19-36.
10. **Dolashka-Angelova P., Stoeva S., Hristova R., Schuetz J., Voelter W.** (2000a) *Spectrochim. Acta* **56** 1985-1999.
11. **9. Dolashka-Angelova P., Dolashki A., Stevanovic S., Hristova R., Atanasov B., Nikolov P., Voelter W.** (2005) *Spectrochim. Acta* **61**, 1207-1217.
12. **Dolashka P., Genov N., Parvanova K., Voelter W., Geiger M., and Stoeva S.** (1996) *Biochem. J.* **315**, 139-144.
13. **Lieb B., Altenhein B., Mark J.** (2000) *J. Biol. Chem.* **275**, 5675-5681.
14. **Markl J.,** (1986) *Biol. Bull. (Woods Hole)* **171**, 90-115.
15. **Privalov P. L., Khechinashvili N. N., Atanasov B. P.** (1971) *Biopolymers* **10**, 1865-1890.
16. **Van Holde K. E., Miller K. I.** (1995) *Adv. Protein Chem.* **47**, 1-81.